Scott's Hollow excavation, Salehurst, East Sussex

Excavation of an ironworking site at Scott's Hollow, Salehurst, East Sussex – an interim report Judie English, David Lea and Jonathan Prus

Effects of furnace clay losses on bloom yields Alan F. Davies

Smelting processes and bloomery iron yields Alan F. Davies

Volume 36

Second Series, Part II

2016

Wealden Iron

WEALDEN IRON RESEARCH GROUP

Bulletin No. 36 Second Series, Part II

2016

CONTENTS *Page No.*

Excavation of an ironworking site at Scott's Hollow, Salehurst, East Sussex – an interim report
Judie English, David Lea and Jonathan Prus 3

Effects of furnace clay losses on bloom yields Alan F. Davies 20

Smelting processes influences on bloomery iron yields
Alan. F. Davies 29

Index 50

Honorary Editor
David Crossley, 5, Canterbury Crescent, Sheffield, S10 3RW

Honorary Secretary
Dr Judie English, 2, Rowland Road, Cranleigh, Surrey, GU6 8SW

ISSN 0266-4402

www.wealdeniron.org.uk

EXCAVATION OF AN IRON-WORKING SITE AT SCOTT'S HOLLOW, SALEHURST, EAST SUSSEX – AN INTERIM REPORT

Judie English, David Lea and Jonathan Prus

Background

Bob Turgoose, a member of the Wealden Iron Research Group and owner of woodland south of Robertsbridge reported that he had found and partially excavated a structure which was in an area where slag had been located and which was probably related to iron production. He requested assistance in completing the excavation and assessing the evidence for iron working in the immediate area.

Topography, geology and present land use

Scott's Hollow lies within an area of mixed coniferous and deciduous woodland historically known as Wellhead Wood and part of Lordship Wood. The area under study covers some 200m x 100m lying east of the road between The Moor and Cripps Corner (A229) and west of a small stream, one of many draining northwards into the Rother (Fig. 1). The ground slopes fairly steeply downwards between the road and the stream. The excavated site lies at 30m OD on the edge of a terrace close to the stream visible on LiDAR (Figure 2) (TQ 77172 23098).

The wood is situated on Ashdown Beds with deposits of Wadhurst Clay and Tunbridge Wells Sand in the immediate vicinity. Excavation indicated that the geology is extremely variable with iron pan, clay, sand and clay with sand mixtures occurring within a few metres.

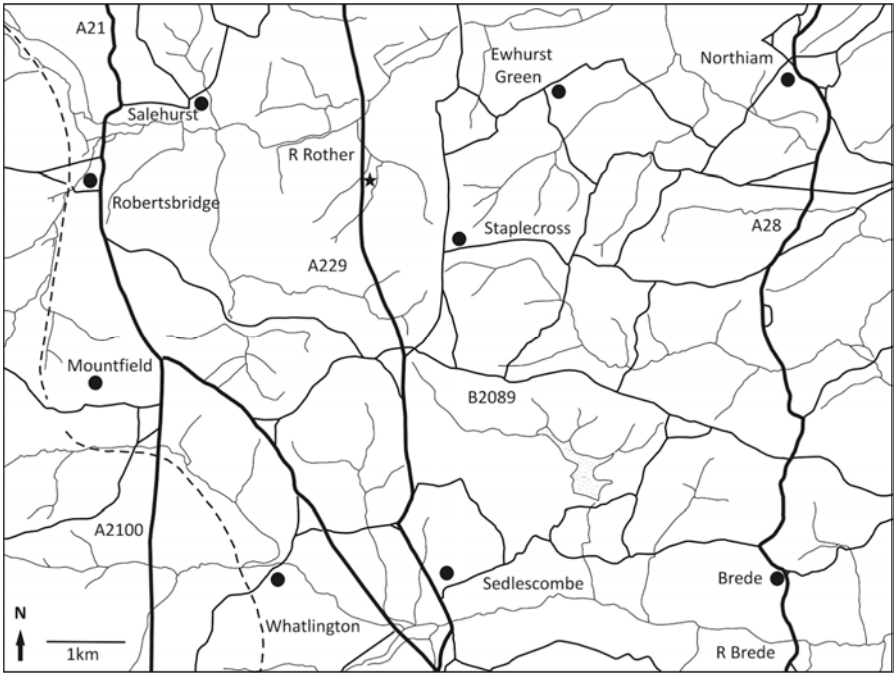

Figure 1 – Location of Scott's Hollow, Salehurst

Analytical and metal detector surveys

A preliminary walkover indicated that a number of earthworks were visible within the woodland and that bloomery slag appeared present at a number of locations. It was therefore decided that an analytical survey of the earthworks and a metal detector survey within a 5m grid should be undertaken and the results are shown in Figs. 3 and 4.

The route of a road running approximately north-south (a) runs through the woodland in the form of a slight terrace. The present A229 originated as a turnpike in 1841; a sketch map dated 1822 and describing a proposed new branch road running close to the pond bay at Park Farm House, Robertsbridge (TQ 751231) does not show a track in Lordship Wood (called on this map Wellinge and Timber Wood) indicating that the surveyed track had gone out of use by that date. Additional slight linear

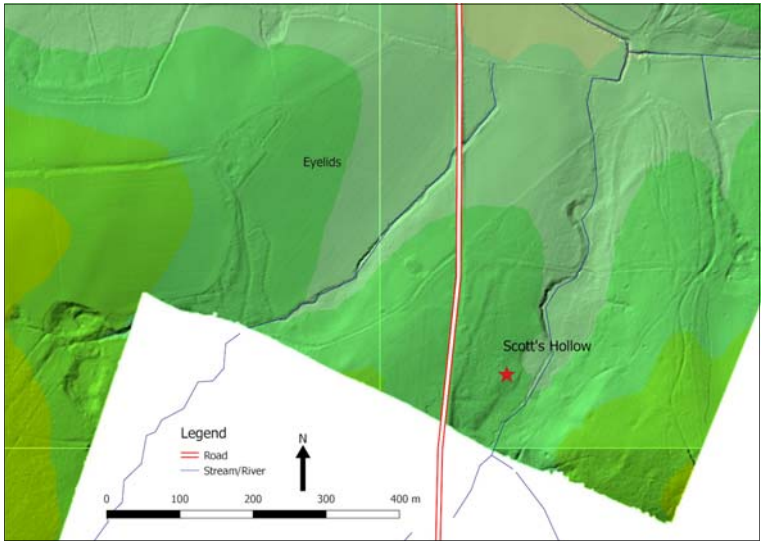

Figure 2 – LiDAR image of Lordship Wood (courtesy of the Environment Agency)

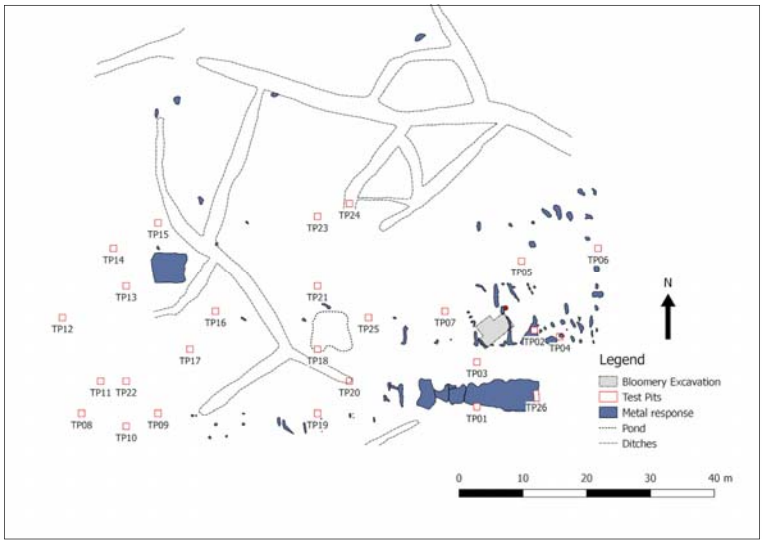

Figure 3 – Results from analytical and metal detector surveys in Lordship Wood

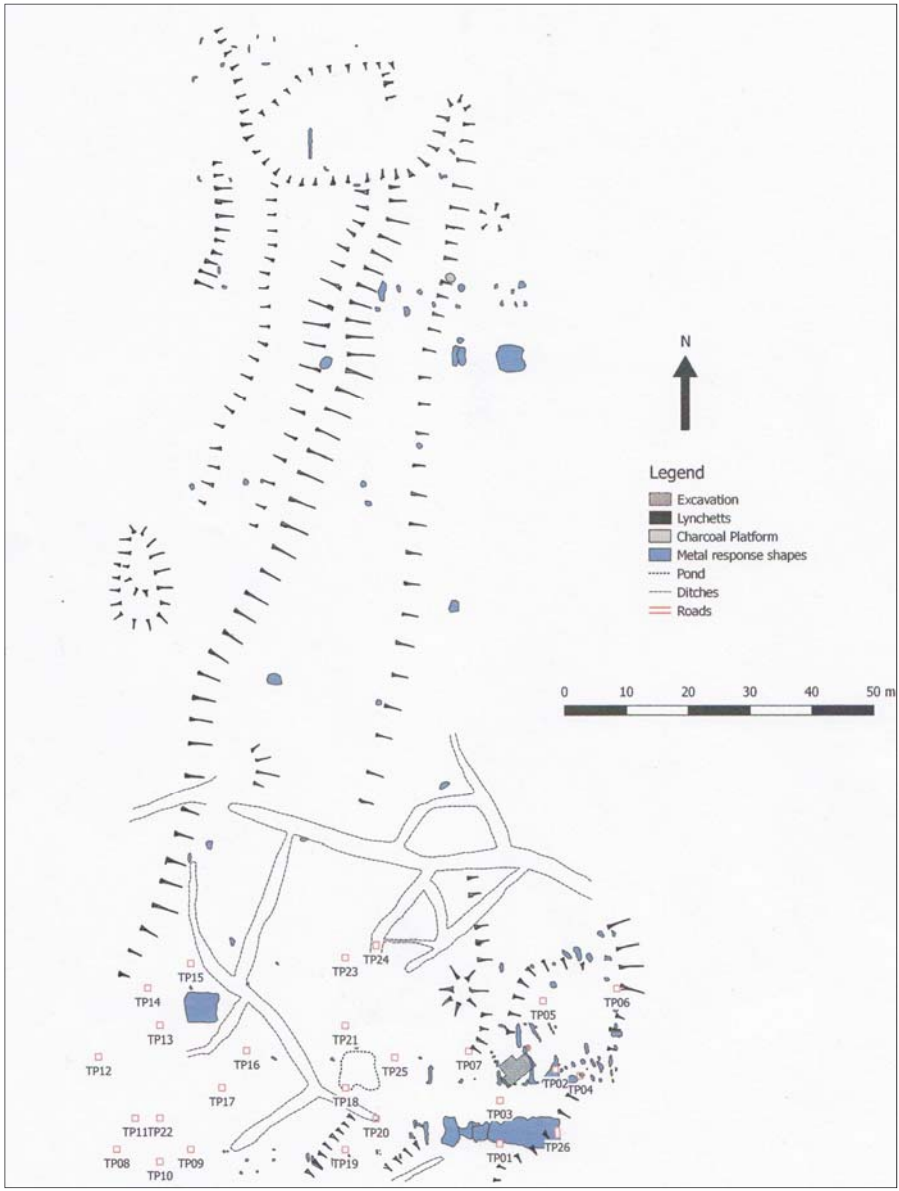

Figure 4 – The excavation area and location of test pits

earthworks (b) may represent parts of a field system of unknown period but presumably pre-dating the use of the land for timber production. A series of channels (c) appears to have been dug for drainage purposes and although all that can be said in terms of dating is that they cut and therefore post-date the possible field boundaries, they seem relatively recent.

The metal detector survey found a number of locations of magnetic material which were considered likely to represent accumulations of slag from iron production.

Test Pits

A total of 26 test pits, each 1m x 1m, were excavated to reveal either undisturbed archaeological contexts or 'natural' geology (Figure 4). Of these 16 were found to contain slag from iron production but an unusually small proportion, less than 10%, could be positively identified as tap slag.

One test pit, TP 04, produced slag together with furnace lining possibly indicating the presence of a bloomery furnace. Indeed, the number of test pits in which slag was found hints at a number of furnaces of unknown date in this piece of woodland. Informal walking in the fields to the west of the A229 also found deposits of slag and there may have been further sites in that area.

Dating evidence was limited to two pieces of pottery. Test pit TP 04 produced a single sherd of Late Iron Age pottery in an apparently undisturbed context and closely associated with bloomery slag. The basal context of test pit TP 02, which did not produce any evidence of iron production but was rich with charcoal and probably located on a charcoal platform, yielded a sherd of 12th/13th century pottery (identified by Luke Barber).

The full results and analyses of the test pitting exercise will be reported elsewhere.

Excavation

Excavation took place at intervals over 2014/15 and was continued to the

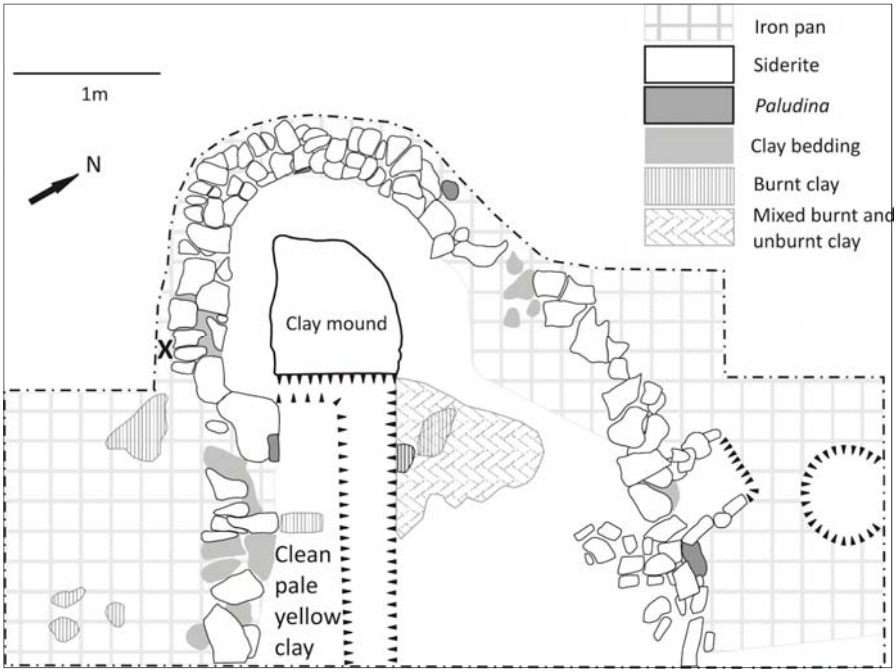

Figure 5 – Excavation plan of the bloomery furnace at Scott's Hollow. X marks the location of a consolidated area of hammer scale (see text)

Figure 6 – Structure at Scott's Hollow under excavation (from the north-east)

Figure 7 – Clay used to bed blocks of siderite at base of wall

point where it was felt that dating evidence and a view of the production processes involved had been obtained. The structure exposed clearly extended outside the trench, particularly down-slope towards the stream but in this direction work was precluded by the presence of a number of trees (Fig. 5).

The furnace was constructed on 'natural' pale yellow, very fine, sandy clay which had been exposed by cutting into the edge of an iron pan and removing a semi-circular portion. This remarkably hard pan, between 20 and 30cm thick, forms a terrace which is visible above ground running roughly parallel to the stream (Fig. 2).

Constructed on the cut edge of the iron pan and stretching eastwards off the edge is a curved wall primarily of slabs of poor quality siderite ore with a small amount (<5%) *Paludina* limestone (Figure 6). The bottom course of the wall had been bedded onto the iron pan using a 1-2cm-thick layer of fine, sandy yellow clay and the bottom four or five courses were similarly sealed (Figure 7). Where the wall survives to a higher level the top courses were of dry stone construction. The majority of slabs and the clay bedding between them in this main, western, portion of the wall were intensely magnetic on the side facing inwards towards the furnace but a small number in the upper courses showed magnetic responses only on the outer side. This would appear to indicate either that the wall had been repaired and some of the slabs reversed or that they had been incorporated into this wall after exposure to heat elsewhere. The lowest course of the wall and the (presumed but not exposed) cut face of the iron pan were covered by a layer of furnace lining – a clay layer plastered against the wall with a slag altered layer facing the clay mound.

Within this semi-circular portion of the wall was a mound of clay which showed extensive but incoherent signs of having been exposed to

high temperatures. Although the mound was half sectioned no internal structure was apparent except at its base and it seems likely that it represented the remains of a collapsed furnace superstructure. The collapsed structure had fallen eastwards, down-slope, and the area to that side contained two elements which enable some comment on the nature of the construction. Firstly, about 20 slabs of clay were found which had been roughly formed into squared blocks, some of which had holes in the ends which could have been used to pin them together with wooden pegs (Fig. 8). There was no consistent size but most were in the order of 20 x 12 x 8cm; although fired when found it is not possible to say whether or not they had been fired prior to use in the structure. These may have formed the lower portion of the furnace superstructure on its eastern side where both the iron pan and slab wall were absent. Also located were a small number of large (more than 30cm diameter) lumps of un- or minimally fired clay with tunnels some 3-6cm diameter running through them (Fig. 9). These had presumably housed a light timber framework although the scantling of the timber precludes a tightly woven wattle.

No details of the form of the superstructure, including the presence of any tuyere holes were recovered and it is uncertain whether there was a dome or a shaft. However, a substantial layer of furnace lining was found attached to the lower courses of the wall indicating that a number of presumably successful firings had taken place (Fig. 10). A slight inward curving of the furnace lining inside the wall suggested a somewhat low structure, perhaps no more than 40cm high. In the space between the clay mound and the wall a slag base was exposed, with a void below it at the bottom of which could be seen a further slag base. At the front, eastern side of the clay mound what was probably the upper of these two hearth bases was found and below it a context whose composition comprised mainly a sand/silt loam with some granular slag and about 22% charcoal. It was not considered worthwhile to try to excavate further in this area due to the inflow of water.

To the north of the furnace the iron pan had been pierced by two holes. One, circular in shape, had been packed with slabs of siderite, which were keyed into the wall probably to support a square-sectioned post (Fig. 11). The other larger circular hole was free of any packing material.
Packed immediately against the outer side of the wall (location X in Fig.

Figure 8 – Low temperature fired blocks of clay from superstructure of furnace

5) was an area of consolidated hammer scale; none was found between the stones of the wall and it appears to have accumulated after its construction.

Discussion

There is clear evidence that of more than one of the processes involved in iron production took place either by adaptation of the excavated furnace or in the immediate vicinity. Much of the evidence relates to smelting using a bloomery furnace but the presence of consolidated hammer scale located outside, and accumulating post construction of, the stone wall suggests smithing of the bloom to produce bar iron. In addition two types of slag were present which could be differentiated chemically and did not relate to the use of variable sources of ore. This is further discussed below.

Although aspects of the composition of the superstructure of the furnace can be described – a base of clay 'bricks' bearing an upper portion of clay supported by wattle – it is not possible to be certain whether it formed a dome or a shaft, although the former is considered more likely (see below).

The two features to the north of the furnace, piercing the iron pan, can speculatively be identified. The proximity of the square hole with the remains of packing material to the furnace may have supported an anvil post. A stone anvil post was found at the Early Iron Age site at Kestor on Dartmoor (Fox 1954) but a timber post, possibly of oak but more likely of elm (Hector Cole pers. comm.), is probable. The round hole may have

Figure 9 – Unfired clay lumps with probable holes for a wattle support from the superstructure of furnace

held water, possibly in a vessel, either for quenching the bloom or for sprinkling the bloom to facilitate slag removal (Schubert 1957), similar purposes to those suggested for the drip pit found at Kestor (Fox 1954).

The period of operation of this site is uncertain but will be clarified when 14-C dates on a number of pieces of charcoal are to hand. In the meantime a single sherd of pottery, recovered from a secure context below one of the large lumps of unfired clay close to the furnace provides a guide. This is probably from a flagon made in the Otford area of Kent and dateable to c.70 – 200AD. If this is correct the site joins approximately 20 known within a radius of 10km including the major production centres of Beauport Park and Oaklands. The main structure is comparable with the iron smelting furnace excavated in Minepit Wood, Rotherfield (Money 1974) considered from the pottery sequence to have been in operation between the mid- to late-1st century AD and the late 2nd century AD, broadly contemporary with the single sherd found at Scott's Hollow. Because of the similarities with Money's RB site members of the group have revisited Minepit Wood and made a slag sample which will be analysed in due course. A key research objective is to see if the slag there has the same characteristics as the Scotts Hollow slag.

The multiple hearth bottoms indicate that at least two successful firings took place in the structure but the large lumps of unfired clay which appeared to have come from the superstructure suggest that the site was abandoned after the dome had been constructed but before it had been fired, possibly because it collapsed. At least one other bloomery furnace existed close-by – whether contemporary or not is unknown, but

Figure 10 – View of area between clay mound and wall showing furnace lining and furnace bottoms

many more sites probably remain to be located here and in the immediate vicinity. The Late Iron Age pottery found in TP 02 suggests earlier activity within the wood probably also associated with iron production.

The structure excavated lies immediately adjacent to a platform, apparently cut into the slope, and test pit TP 04 produced over 1m depth of charcoal rich soil. The 12th/13th century pottery sherd from the base of the test pit indicates medieval charcoal production, probably related to the ownership of the woodland by the Cistercian abbey at Robertsbridge founded in 1176.

Although small amounts of bloomery slag were found throughout the woodland neither the test pits nor the excavation yielded large amounts of slag and it seems clear that much must have been removed, possibly during construction of the turnpike road. Such re-use was widespread in the 19th century with comments that 'cinder-beds at Sedlescombe have been thoroughly worked out' (Rock 1879) and, referring to the B2244 which passes Scott's

Figure 11 – Vertical view of the packed post-hole which may have supported an anvil post

Hollow "609 loads of cinder were taken from Footland Farm for the making of the Turnpike road at 2d per load" (Lucey 1978 as utilised by Cornwell & Cornwell 2013).

An interpretation of the structure at Scott's Hollow

Jonathan Prus

We now have some hundreds of Portable X-Ray Fluorescence (PXRF) measurements for Wealden slag from fifteen sites (Flint *et al.*, forthcoming). The sites were assumed to be of a bloomery production type.

A histogram of the iron contents of the slag samples produces a striking result (Fig. 12)

There is a range of values for iron in slag from over 50% to 32%. 50% is

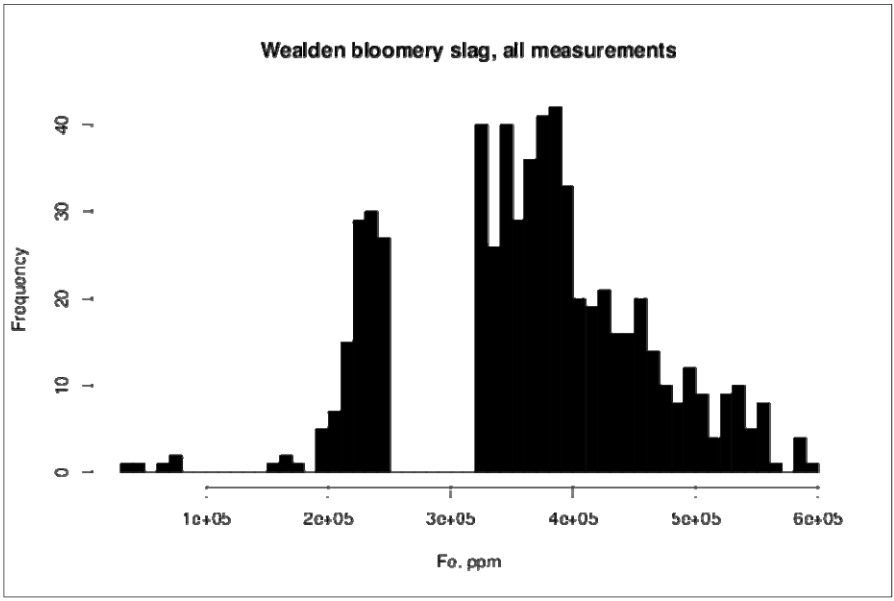

Figure 12 – Wealden bloomery slag – all measurements

near to the mean value for roasted ore found *in situ*. (Slag with this high-iron content has probably passed through the system without change to its bulk composition, although the oxidation state of some of its constituents may have changed.) There is a sharp break at 32% with no readings between 26 and 32%. A histogram of the measurements in the range 32-50% appears to shows a left-skewed non-normal distribution and has a mean iron value of about 42%.

The obvious inference is that slags with iron contents of 26% and below are formed by a different process. This is supported by experimental work (Crew and Serneels, 1997) and by the measurement of archaeological slags (Eschenlohr and Serneels, 1991) in the Jura. The latter proposed a form of furnace for this secondary process but were unable to identify a specific furnace linked to it. It must be noted that the iron content reported by Eschenlohr & Serneels for the secondary process is above 26% (reported as oxides but implying 42%>Fe>28%). Their values for primary smelting tap slag overlap this range but are clearly separate on a ternary diagram (Fe-Al-Si).

The Weald slags with Fe<26% are characterised by elevated silicon and calcium levels. This is consistent with the use of white sand as a flux, in a process where bloom is converted into bar or other usable forms. It is also consistent with the incorporation of additional calcium from fuel ash during secondary processing. Although the Scott's Hollow site is unexpectedly rich in manganese there is no evidence that manganese-rich material from the immediate vicinity was added to the mix in this process. The latter observation rules out the possibility that the high-silica slag resulted from ordinary primary smelting slag running over the floor of the working area.

The slag in question is similar in appearance to other run slags, but that from Scott's Hollow has a slightly glaucous appearance on fracturing. It is not yet known if this colouring is significant.

Hammerscale

Hammerscale is present in all soil samples taken from the study site. It is composed of sharp plates somewhat less than 1mm in thickness, often ending in acute angled points, a type that is associated with bloom-smithing. There are also some finer plates of material more closely

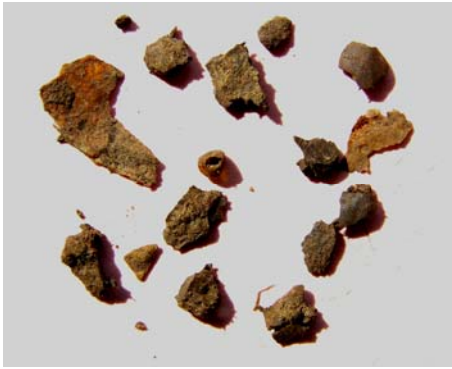

A small selection of hammerscale types from the vicinity of the Scott's Hollow structure. The relative abundance of different types is not reflected in this selection. The colour contrast has been exaggerated to make the differences clear. The natural colour is predominantly grey. (Photograph by Brian Herbert)

resembling modern mill-scale (Fig. 13). There is a possible spherule (centre fragment in Fig. 13: this is approximately 1.5mm across. Attention to its shadow reveals that it is probably hollow and forms a translucent shell). The object is possibly a product of forge-welding (Dungworth and Wilkes 2007). In general the presence of a hammerscale layer suggests that blooms could have been converted into bar iron. Spherules may mean that the fabrication of more complex items (such as edged tools or larger composite objects) happened at Scott's Hollow.

The corollary of a process that uses additional silica as a flux is a hammering process that closes voids and fractures in the iron, making hammerscale and ejecting slag. Although hammerscale is found across the site, it also exists as a discrete stratum (a concretion) in at least one phase of the site's operation (see above).

In order to make hammerscale there must have been an anvil (of some description) within the working area.

Slag morphology

The canonical form for bloom-smithing slag is bun-like in shape and size (Eschenlohr and Serneels: "*calottes*"). It is not clear whether this is based strongly on the evidence or is an inference from the characteristic shapes of other smithing slag. Most of the slag of interest here has flowed. This is consistent with bloom-smithing in a slag bath that is augmented with sand and which was not allowed to exceed a certain depth.

Location of 'secondary process' slag finds

The largest deposit of slag found within 80m of the excavated structure was in TP26, about 10m SE of the excavation. 24 specimens were taken for PXRF analysis. Of these 16 are of the secondary type. There was no visible stratigraphy in the slag stratum from TP26 and the relative vertical positions at which the different types were found are unknown.

19 specimens were taken from TP4. Of these 7 are of the secondary type and 6 specimens were taken from context 102 of the excavation of which 2 were of the secondary type.

Phasing

The presence of primary smelting slag is additional evidence for a multi-phase use of the area, though not necessarily the site excavated.

For the purposes of comparison, secondary type slag occurred in seven of the fifteen sites represented in the histogram above. In no other case did it occur at the frequency observed at Scotts Hollow.

The horseshoe-shaped revetment in the excavated structure is made of a hard rock that exfoliates like the sideritic iron ore typical of the Weald. It turns out to have a moderate siderite content. It contains too much silica to be a good smelting ore. This set of stones may be interpreted as ore discarded by a master smelter who recognised the sparkle of excess silica as something that caused smelts to fail. These stones are strong evidence that ore was collected for smelting somewhere nearby in a period prior to the building of the excavated structure.

The presence of primary smelting slag (and a tiny amount of roasted ore) is inconclusive evidence that there was a bloomery there before the construction of the later furnace. The predominance of primary smelting slag in TP4 is strong evidence that there was a bloomery nearby during some stage of the site's use.

Possible form of the excavated structure

For evidence of the working structure in its last phase we have:

- a low stone-built semi-circular revetment, mortared with a silt-clay mix, built onto a hard flat surface cut into the manganese-rich iron pan
- lining made of a fine-sand mix bound with perhaps 20% to 40%

clay

- internal diameter about 700-800 mm.
- an all-round slag-attacked base up to a level of +/- 200 mm.
- potassium glass vitrification of the lining above +/- 200 mm. This glass is doped with iron at approximately the same percentage found in the lining
- tumbled rough blocks with a variable *voussoir* shape
- no evidence of an aperture through which an air blast could be introduced.

This is consistent with a low, domed structure containing a smithing hearth. The air-blast could have been blown from the top of the fuel bed, avoiding the waste of energy involved in carbon monoxide production. The dome could have acted as a reverberator for radiant heat.

Acknowledgements

We would like to thank all those who took part in the metal detector survey and the excavation, particularly Gerry Crawshaw and Bob Turgoose, and Vivienne Blandford who undertook some of the site drawing. Much gratitude is also due to Bob Turgoose who discovered the site and, as landowner, invited and facilitated the fieldwork.

Bibliography

Cornwell, K. and Cornwell, L. with Padgham, D., 2013, 'Footland Farm, Sedlescombe: a geophysical survey of the iron production complex and its transport links', *Hastings Area Archaeological Research Group Journal*

Dungworth, D. and Wilkes, R., 2007, An Investigation of Hammerscale. Research Department Report Series No. 26/2007. English Heritage. Portsmouth

Eschenlohr, L. and Serneels, V., 1991, *Les bas fourneaux mérovingiens de Boécourt-Les Boulies (JU/Suisse)*, Cahier d'Archéologie Jurassienne nº 3, Office du Patrimoine Historique et Société Jurassienne d'Emulation, Porrentruy.

Flint, A., Leigh, G.L., Prus, J. and Salvage, J. (forthcoming) Quantitative Aspects of Iron Extraction in the Sussex Weald.

Fox, A., 1954, 'Excavations at Kestor: an Early Iron Age settlement near Chagford, Devon', *Rep & Trans Devon Assoc for the Advancement of Science , Literature & Art*, **86**, 21-62

Lucey, B., 1978, *Twenty centuries in Sedlescombe: an East Sussex parish*, London: Regency Press

Money, J. H., 1974, 'Iron Age and Romano-British iron-working site in Minepit Wood, Rotherfield, Sussex', *Journal of the Historical Metallurgy Society*, **8**, 1-20.

Rock, J., 1879, 'Ancient cinder-heaps in East Sussex', *Sussex Archaeol. Coll.*, **29**, 167-180.

Serneels, V. and Crew, P. 1997 *Ore-slag relationships from experimentally smelted bog iron-ore,* in P. and S. Crew, Early Ironworking in Europe, archaeology and experiment, vol. II Experimental and Technical Studies, International Conference Plas Tan y Bwlch, 19-25 Sept. 1997, Plas Tan Y Bwlch.

Schubert, H. R., 1957, *History of the British Iron and Steel Industry 450BC – 1775AD*, London: Routledge & Keagan Paul, 28.

EFFECTS OF FURNACE CLAY LOSSES ON BLOOM YIELDS

Alan F. Davies

Introduction

Aims and Background

During summer 2015 the WIRG smelting team completed smelts 8, 9 and 10. Smelt burden data plus bloom and slag quantities for smelts 8 and 9 are compared with results from a computer based bloom yield prediction model. Both smelts used the same siderite ore (BWS 1), charcoal and furnace clay materials and essentially the same smelting process conditions. This article shows how differences between actual and 'ideal' bloom yields can be related to furnace clay losses to the melt.

Model Summary

Full details of the model can be found in Davies (2015). However as a summary the premise built into the model requires calcined ore to provide more than a 4:1 ratio of iron to silicon to ensure surplus iron over slag forming needs to give a bloom. Wealden ores, with typical ratios of 7:1 to 14:1, achieve good bloom yields with good furnace management. During smelting, however, extra silica (plus other minerals) over that from the ore enters the smelt from clay furnace wall liquation or erosional losses. More slag is produced leaving less wüstite overall for metallisation to iron. High take up of extra silica causes a low or even a 'no bloom' yield.

Figure 1 shows an example of slag grain boundary permeation at 2mm deep in a bloomery furnace wall sample. At the surface there is a higher proportion of wüstite in the slag whereas at 4mm and deeper slag is more glass-like with no free wüstite.

Model inputs are a combination of burden weights and mix ratio, ore and charcoal mineral contents and qualities, usage rates, furnace wall composition, gases ratio, smelting time and calculated blow rates. These,

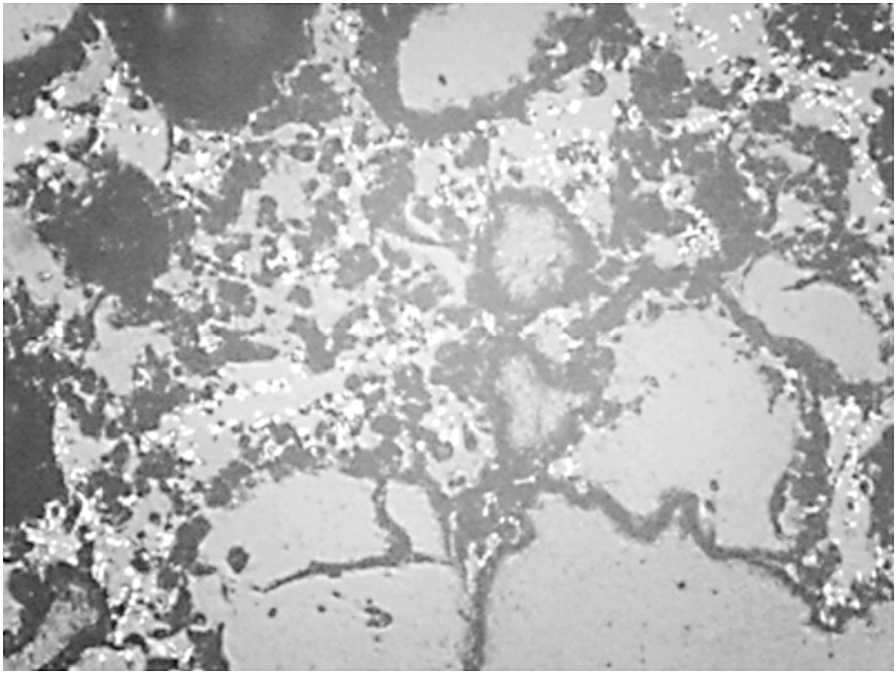

Figure 1 – White Wustite in Fayalite Slag permeating larger grey Silica Grains (x100)

with consistent furnace management, provide a means to predict smelt bloom weight, yield and final slag weights. The model also combines variations in ore calcining extent in a standard burden mix ratio or yield changes from varying effects of lime quantities in ore.

Fig. 2 shows how model processes link smelting inputs to smelting outputs. The model compares predicted bloom weight and yield % values with actual outputs from field data. Firstly it calculates an ideal bloom weight, yield and slag quantities. Secondly it determines the weight of any additional furnace clay loss to the melt to align model outputs with actual smelt values.

Smelting Conditions

The furnace is top charged with single 20mm diameter tuyere air entry 90°

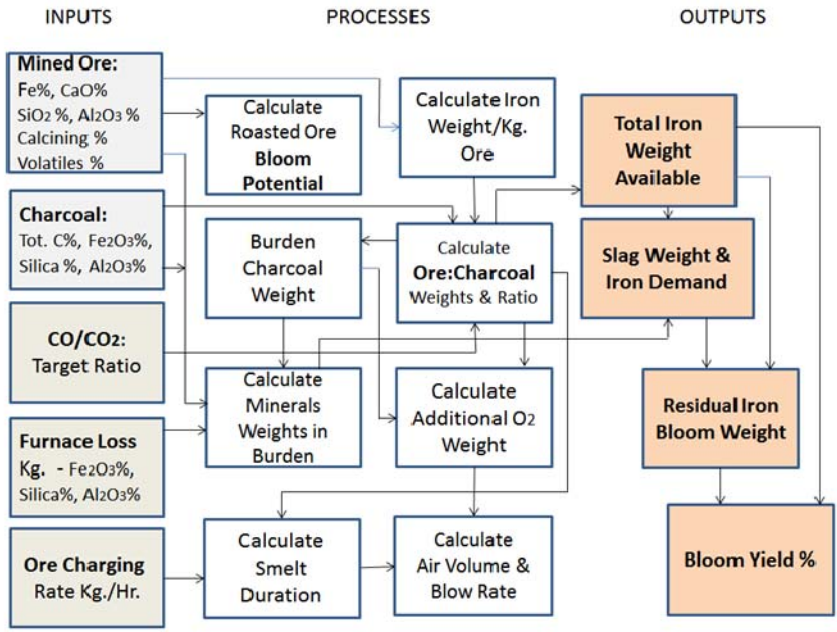

Figure 2 – Summary of Model Inputs, Processes and Outputs

from the hearth position, 22cm above the furnace bottom and 20° declination, via flow meter from an electric blower. Hearth level furnace diameter is 45cm giving a blowing cross-section of about 1,590cm^2. Both smelts followed essentially the same smelting plan.

Charging & Blowing Rates

The ore quantity used and, therefore, smelting times were slightly less for smelt 9, compared with smelt 8. Smelt 9 used 2kg burden loads of charcoal every 15 minutes followed by 2kg crushed roasted ore as 4 x 500gm charges sprinkled over charcoal over 15 minutes. The blowing rate was varied stepwise during smelting with an average of about 11l/sec (0.42l/min./cm^2) for each.

Slag Tapping

Smelt 8 gave an initial small run and a second copious run of tap slag.

Apart from a short trickle smelt 9 gave no slag run owing to a viscous slag, found by probing, although a bloom had formed. Later slag fluidity analyses indicated furnace temperature was likely marginally low for a good slag flow.

Output Slag Types/Bloom

Slag samples from each smelt were collected and weighed: Tap Slag from two furnace taps for smelt 8 but none from smelt 9, raked out Furnace and Cinder Slags plus some Bloom Slag hammered off blooms after extraction. Bloom weights recorded. Post smithing weights for pan and run slags and final billet weight from each smelt were recorded.

Some estimates of slag quantities were made by smelting team to

Specification %	Calcined Ore	Charcoal	Furnace Clay
Total Iron as Fe	49.53	0.74	3.64
Carbon	-	98.35	-
Fe_2O_3	66.73	1.06	5.2
FeO	3.64	0	0
Silica	14.24	0	87.37
Alumina	5.09	0.28	7.71
Lime	5.02	0	0
Magnesia	3.19	0	0
Manganese Oxide (MnO)	0.24	0	0
Volatiles	1.73	0	0.76
Calcining	95%	-	-

Table 1 – Mineral Contents of Burden Inputs and Furnace Structure

account for slag still adhering to furnace walls and for some sieve losses of Cinder Slag fines. Small corrections were made for total Bloom Slag. Any lumps of unreduced ore were separated and weighed to give the net ore weight used in smelts.

Acknowledgements
Thanks must go to members of the smelting team for collecting, sorting, weighing slag quantities and providing samples for analyses following each of the smelts and bloom smithing.

Findings

Input Burden Materials and Compositions:
Analysis results for samples of ore, charcoal and furnace clay used are shown in Table 1.

Output Slags and Weights
Table 2 gives weights for smelt 8 smelting and forge slag types, bloom and billet. An identical technique was used for smelt 9 slags and bloom although tap slag was included with the raked out slag weight.

Fig. 3 shows, for smelt 8, raked out Furnace + Cinder slags weights made up about 63% of the total recovered slags with tap slag representing almost 30% of the total and balance of bloom slag.

Model Outputs and Actual Smelt Results

Predicted and Actual Gross Bloom Yields
Table 3 compares two sets of results. The upper part of the table shows outputs weights and yield% values whilst the lower section shows smelting process conditions. A very high recovery of slags was achieved by smelt team members.

The first data column of each smelt shows Base (Ideal) results from burden materials without any additional clay contribution from furnace structures. Upper highlighted rows show that the Ideal bloom would be

Origin:	Tapped	Raked Out		Detached	Extracted	Recovered		Smithed
Slag Type:	Tap Slag (Avg.)	Cinder Slag	Furnace Slag	Bloom Slag	Bloom (Cleaned)	Forge Pan	Forge Run	Billet (C = 0.02%)
Weight Kg.	5.8	11.2 + Est. 2Kg.		2Kg. (Est.)	4.35	2.8		1.85

Table 2 – Smelt 8 - Recovered Weights of Slag Types, Bloom and Billet

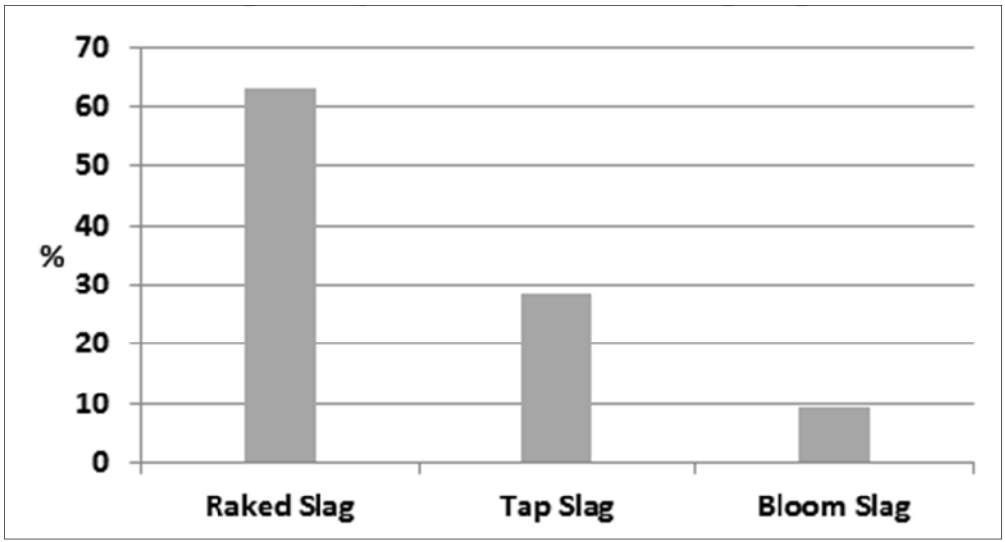

Figure 3 – Smelt 8 - Weight Proportions of recovered Smelt Slags

OUTPUT RESULTS:	Smelt8 Base (Ideal)	Smelt8 Actual Smelt	Smelt 8 Model (Predicted)		Smelt9 Base (Ideal)	Smelt9 Actual Smelt	Smelt 9 Model (Predicted)
Total Iron Available (Kg.)	13.3	13.5	13.4		12.1	11.9	12.2
Silica Available (Kg.)	3.8	n.m.	5.4		3.4	n.m.	5.7
Slag (Kg.)	15.6	21.0	21.1		14.1	24.5	22.0
Iron in Slag (Kg.)	6.1	n.m.	9.03		5.5	n.m.	9.7
Iron Available in Bloom (Kg.)	**7.2**	**4.35**	**4.35**		**6.6**	**2.45**	**2.45**
Gross Bloom Yield (%)	**54.2**	**32.2**	**32.6**		**54.3**	**20.6**	**20.1**
Smithing Loss (%)	58	58	58		31	31	31
Post Smithing Billet Weight (Kg)	3.0	1.85	1.83		4.5	1.7	1.7
Post Smithing Billet Yield (%)	22.8	13.7	13.7		37.4	14.3	13.9
PROCESS RESULTS:							
Extra Furnace Clay (Kg.)	**0**	6 (Est.)	**1.8**		**0**	**n.m.**	**2.57**
Furnace Clay Loss as % of Ore Wt.	0	n.m.	6.8		0	n.m.	10.7
CO/CO_2 Ratio	5.0	n.m.	5.0		5.15	n.m.	5.15
Ore/Charcoal Ratio	1.0	1.0	1.0		1.0	1.0	1.0
Ore (Kg.) - (nett used)	26.5	26.5	26.5		24.0	24.0	24.0
Charcoal (Kg.)	27	27	27		23.9	23.9	23.9
Avg. Blowing Rate (L/Sec.)	10.2	11.4	10.2		10.5	n.m.	10.9
Avg. Blowing Rate (L/min./cm^2)	0.38	0.42	0.38		0.40	n.m.	0.41
Smelt Duration (Hrs.)	5.5	5.5	5.5		4.8	4.1	4.8

Table 3 – Comparison of Model and Actual Results for Smelts 8 and 9

n.m. = not measured in smelt

7.2kg and 6.6kg for smelts 8 and 9 respectively giving ideal Gross Bloom Yields of 54.2% and 54.3% respectively.

Additional Clay

However differences between Base values and Actual Gross Bloom Yield% values of smelt 8 - 32.2% and smelt 9 - 20.6% respectively, shown in the middle column of each set, represents iron lost to extra slag from more clay entering the melt. These clay quantities 1.8kg and 2.57kg for smelts 8 and 9 respectively are highlighted in the lower section of right hand column. These values, calculated to align model bloom weight to actual values, represent about 7% and 11% respectively of burden roasted ore weights. The higher proportion of silica in smelt 9 plus progressive wüstite loss from metallisation would increase slag viscosity and reduce bloom growth rate and yield as found. This effect with marginally low temperature for tapping smelt 9 prevented a good tap slag flow.

Post Smithing Yields and overall Efficiencies

Post Smithing results show that the final overall Billet Yields are 13.7% and 14.3% from the total available iron in smelts 8 and 9 respectively. Extending this point the available iron in well calcined ore is close to 50% of weight. So the average final billet yield now becomes about 7% of *calcined ore* weight. As the final step the yield from mined siderite ore (32% volatiles loss during full calcining) gives 4.8% metal yield from *mined ore* weight. In contrast, no additional clay would give yields of 8% and 13% from mined ore for smelts 8 and 9 respectively.

Conclusions

Modelling helps to explore and quantify the effects of interactions and changes within a furnace smelting system. Within the basic premise of the model these findings show that each smelt, with good management, had an ‘ideal’ potential Gross Bloom Yield of 54% of maximum iron available from siderite ore used and other burden inputs. The balance of iron is found in the slag.

However in practice actual yield results of about 32% for smelt 8 and 21% for smelt 9 realised only a portion of this ideal result. Each smelt showed the effects of additional clay pick-up giving a lower bloom weight, yield and increased slag quantity. This clay pick-up weight represented 7% and 11% respectively of smelt burden ore weight.

Measures like these provide evidence into the archaeological record for assessing historical bloomery and smithing productivities. Analysis shows the metal iron weight available after smithing can represent easily only about 5% of the original mined siderite ore weight. Practically, but not for these two trials, recycling of smithing wastes or using slightly more calcareous ores or even furnace lime additions may help boost metal yields.

Results show also how, even starting with the same inputs, specifications and seemingly similar smelt management methods, process variations nevertheless led to different weight proportions of clay pick-up and bloom yields. Generally, with best intentions of applying common practices, even minor differences in quantities and processes lead to significant differences in final yields.

Bibliography

Davies, A. F., 2015, 'Exploring How ore bloom potential and other factors influence iron yields', *Wealden Iron*, Bulletin of the Wealden Iron Research Group, 2nd. ser., **35**, 13-29.

SMELTING PROCESSES INFLUENCES ON BLOOMERY IRON YIELDS

ALAN F. DAVIES

Introduction

During summer 2015 the WIRG Smelting Group undertook smelts 8, 9 and 10. Aims included trialling different furnace air flow rates, slag tapping arrangements and furnace tuyere sizes and entry positions for effects on bloom yields. This article compares results of these smelts and documents the findings in the contexts of ore reduction processes, burden inputs, bloom yields, slag types and mineral contents. Smelting variations in slags viscosities are reviewed for likely influences on bloom formation, metal yields and carbon contents. Findings are consolidated into an *Influence Map* showing how variations in smelting inputs and process conditions can affect markedly bloom yields and qualities.

Acknowledgements

The author would like to thank members of the smelting team for their extensive help and support in producing smelt reports and collecting, sorting, weighing slags, blooms, billets and providing samples for mineral and micrographic analyses.

Summary Results for Smelting Productivity

Smelts burden input specifications and ore:charcoal ratios were constant for the three smelts. Small differences in ore quantities needed different smelt times and air flow rates. Each smelt was managed using essentially the same practices. However smelt 10 experienced three events: a) a larger than usual quantity of residual pre-heat wood and ash in the hearth at the start of the smelt. b) tuyere entry position relocation from furnace side to above hearth. c) air blower generator failure with a 15 minute

delay to set up hand bellows pumping for 1½ hours and deferred bloom smithing. Even so a 71% bloom yield was achieved.

Bloom Yields

Table 1 shows results for the three smelts.

SMELT RESULTS:	Smelt 8	Smelt 9	Smelt 10
Smelt Iron Available (Kg.)	13.5	11.9	9.9
Slag (Kg.) (Weighed+est.)	21.0	24.5	18.6
Iron Available in Bloom (Kg.)	4.35	2.45	7.05
Gross Bloom Yield (%)	32.2	20.59	71.21
Bloom Carbon Content %	0.02	0.42	0.30
Smithing Loss (%)	58	31	-
Post Smithing Billet Weight (Kg)	1.85	1.70	-
Post Smithing Billet Yield (%)	13.7	14.3	-
PROCESS RESULTS:			
Ore (Kg.) - (nett used)	26.5	24.0	20.0
Charcoal (Kg.)	27	23.9	20.0
Avg. Blowing Rate (L/Sec.)	11.4	10.9 (Est.)	8.8 (Est.)
Avg. Blowing Rate (L/min./cm^2)	0.42	0.41 (Est.)	0.33 (Est.)
Smelt (Hrs.)	5.5	4.1	5.0
Iron Drop Rate (Gms/min.)	13.2	10.0	23.5
Tuyere above furnace bottom (cm)	22	22	36
Tuyere Declination	-20°	-20°	-20°
Tuyere Diam. (mm)	20mm	19mm	19mm

Table 1 – Summary of Smelting Results

Whilst net ore quantity used for each smelt decreased slightly as trials were done, corresponding Gross Bloom Yields % values varied significantly especially for smelt 10.

Effect of Tuyere Height

Smelt	8	9	10		R
Gross Bloom Yield %	32.2	20.6	71.21		0.98
Tuyere from bottom (cm)	22	22	36		

Table 2 – Correlation (R) between 'Gross Bloom Yield %' and Tuyere Height

Table 2 shows a high correlation between Gross Bloom Yield% and tuyere height. Whilst this could signify a benefit of tuyere relocation the effects of other changes as contributory factors cannot be excluded.

Bloom Carbon Content

Table 3 shows the results of chemical and metallographic analyses for the average carbon content of small sections of iron from each smelt. Samples for smelts 8 and 9 are taken from consolidated billets. That for smelt 10 is the average value from a bloom slag iron sample with range 0.06%C – 0.61%C

Smelt	8	9	10
Iron Average Carbon%	0.02	0.42	0.30

Table 3 - Smelt Iron Carbon Contents

Ore Reduction

Table 4, after Gupta,[1] shows iron oxides reduced to iron through three stages of oxygen removal above 570°C. Minimum $CO:CO_2$ ratios are given for ore reductions at smelting temperatures.

Forming wüstite (FeO) represents just 30% total ore reduction using a minimum of 25% $CO:CO_2$ ratio in the furnace shaft. Achieving the important third stage metallisation needs a further 70% reduction at higher temperature with a minimum reducing gas ratio of 3.

Oxide Reduction Stage:		1	2	3	
Ore Oxide:	Fe_2O_3	→	Fe_3O_4 →	FeO →	Iron
Total Oxide Reduction %:		11.2	30	100	
Minimum $CO:CO_2$ Ratio @ Deg. C:		0.05 (500°C)	0.25 (1000°C)	3.0+ (1200°C)	

Table 4 – Iron Oxide Reduction Stages and required minimum $CO:CO_2$ Ratios

Slag Types

Four broad types of slag structures were collected after smelting and are shown in Fig. 1. Based on morphology these are: furnace, cinder, bloom and tap slags.

Furnace Slag

This high silica slag looks more a mix of burden materials and forming slags from the upper furnace stack and corresponding to Stage 1

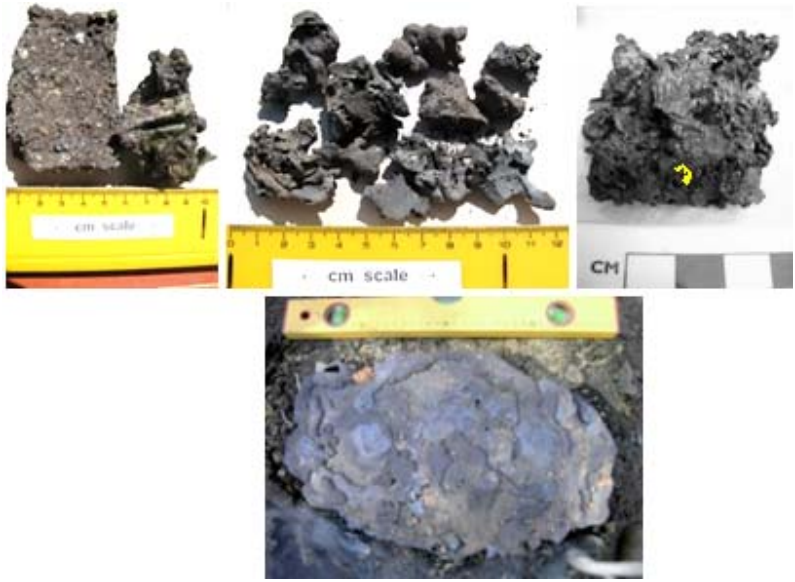

Figure 1 – L to R: Furnace, Cinder, Bloom & Tap Slags

reduction. As found from smelt 8, a glassy slag may form from burden fusing at higher temperature. During smelt 9 a green glassy slag formed on furnace walls above the smelting arch.

Cinder Type Slag

As the burden descends the furnace shaft higher temperatures cause Stage 2 fusion forming wüstite with silica (plus alumina, lime, magnesia and other minor minerals from ore) as black fayalite slag and metal silicates when cold. Moreover there is likely to be more fayalite type slag created from further minerals pick-up by contact diffusion and erosion between furnace clay/silica walls and wüstite.

Cinder and Bloom Slags Metallisation

Microstructures of third stage reduction and metallisation show iron particles nucleating from wüstite and accreting into iron globules.[2] Table 5 shows, from metallography, weight proportions of metallised iron found in samples of cinder and bloom slags.

Using these values gives Figure 2 showing the progress of reduction

Analysed Tot. Fe %	Slag Type	Free Iron Wt.%	Metallisation %	Reduction %
43.08	Smelt 9 Cinder	3	8	36
30.41	Smelt 8 Cinder	20	66	76
38.13	Smelt 10 Cinder	30	79	85
65.88	Smelt 9 Cinder	56	85	90
84.28	Smelt 9 Bloom	77	91	94
60.90	Smelt 8 Bloom	58	96	97
86.43	Smelt 10 Bloom	85	98	99

Table 5 – Ore Reduction and Slag Metallisation

[% Reduction = (% Metallisation x 0.7) + 30]

and metallisation during smelting. As any one cinder sample cannot be placed at a point in smelt time, having been selected at random from a pile after furnace rake out, a 'notional' time scale is used. Doing so shows linearity of reduction and metallisation processes with clustering of samples near the end of the process period where more free iron is seen in samples. Cinder slag can be considered as bloom slag at around 90%+ metallisation.

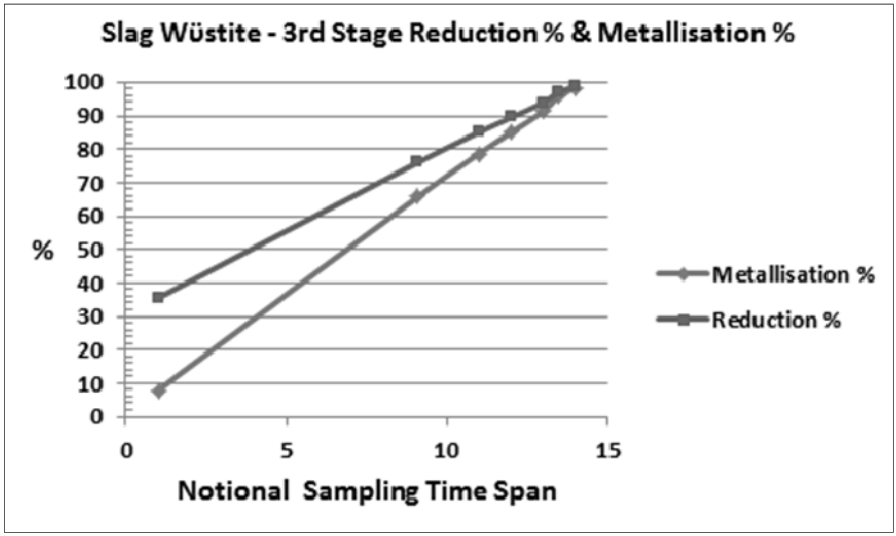

Figure 2 – Reduction and Metallisation of Bloomery Slags

Fig. 3 shows findings[3] from other haematite reduction laboratory trials (using different methods), showing oxides transitions to wüstite and final reduction to iron. Base line axis represents time and gives a useful measure for rate of change. At about 30% reduction degree and also about 30% of reduction time, free iron starts to form and develops to 100% as the reduction degree reaches 100%. These values correspond with findings for the three smelt slags showing likewise 30% reduction before the start of iron metallisation, the third stage requiring a further 70% oxide reduction and linearity of process changes. Moreover it shows that full reduction of wüstite requires about 70% of overall (smelt) time.

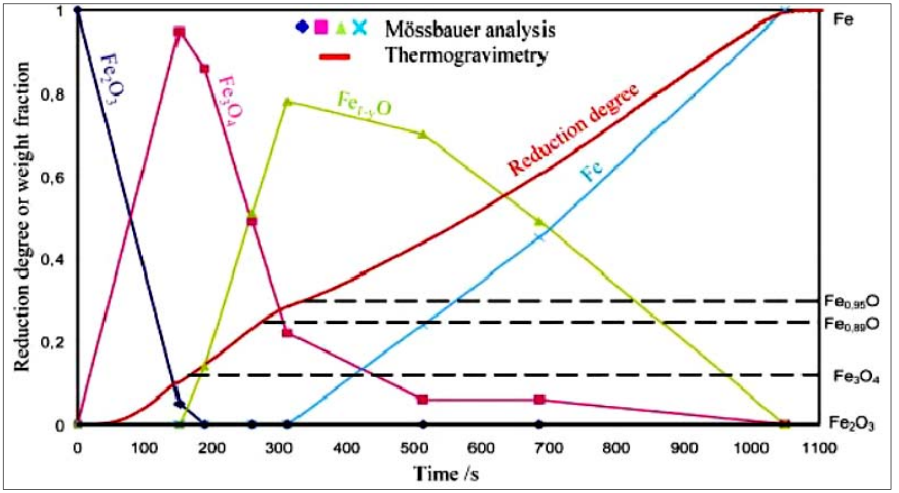

Figure 3 – Oxides Transitions and Reduction to Iron during Haematite Smelting

Tap Slag

Fresh pieces characterised by a grey fairly smooth exterior surface but which overall may show some 'ropey' features depending on temperature, flow and solidification rates during tapping and collection. Fracture surfaces are grey/silvery with fine vesicles near lower surface of slag layer.

Mineral Profiles

Cinder Slag

Fig. 4 compares cinder slag sample mineral profiles from each of the smelts. As described above cinder slag composition evolves during reduction. Therefore analysis of any one piece collected at random from furnace rake out represents just one of a possible range of melt compositions at a state of reduction or metallisation as shown.

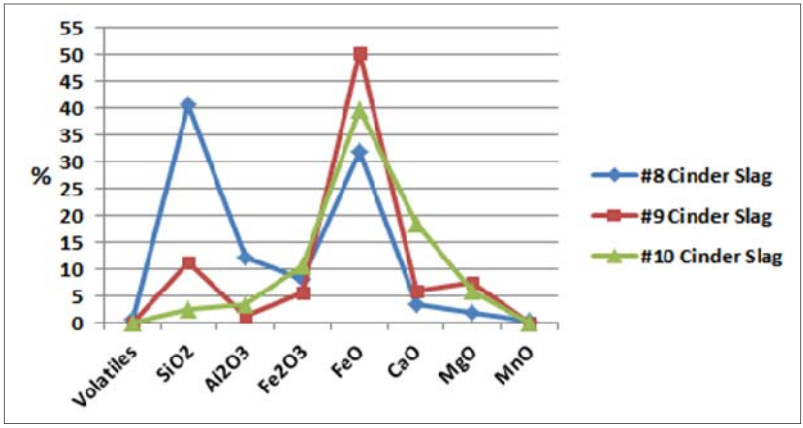

Figure 4 – Comparing Sample Cinder Slag Mineral Profiles

Bloom Slag

Unlike cinder slag profiles, bloom slags samples show, Fig. 5, a much more consistent mineral profile across smelts. Again total iron represents free iron plus that in fayalite expressed as FeO. Total iron content varies around higher values than for cinder slag indicating more reduction and metallisation. Silica and alumina contents converge towards lower values.

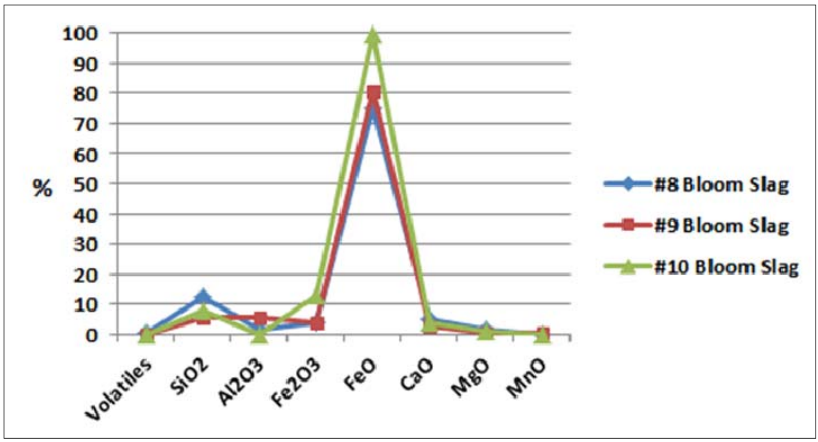

Figure 5 – Comparison of Bloom Slags Mineral Contents

Tap Slag

Comparing tap slag profiles, Fig. 6, shows no free iron, high convergence to about 45% FeO but unlike bloom slags, wider variation in silica and alumina contents.

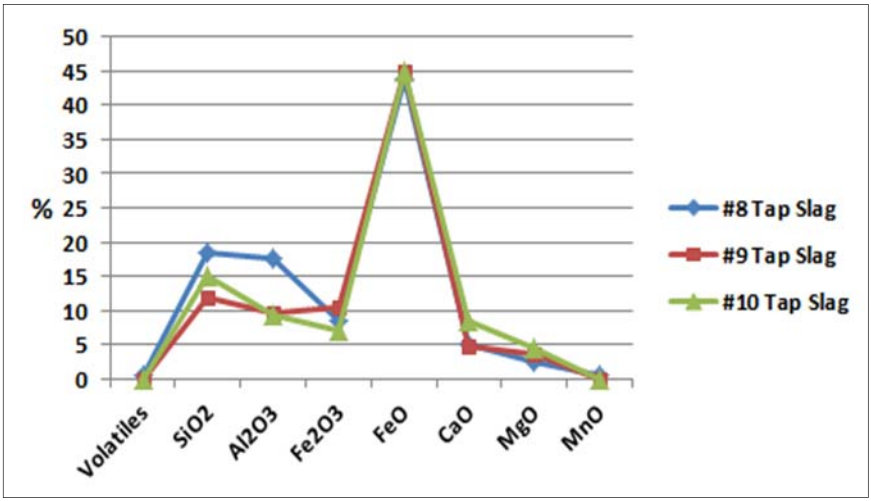

Figure 6 - Comparison of Tap Slags Mineral Contents

Minerals Redistribution

Fig. 7, using smelt 8 as an example, shows how the main input mineral proportions in ore and furnace wall are redistributed across slag types during smelting.

Slag Viscosity Characteristics

Each smelt produced a tap slag of different viscosity. Smelt 8 produced a good flow whereas smelt 9 gave no flow and only a sticky slag on probing. Smelt 10 produced a copious flow of very fluid slag. With such variation, slag viscosities across smelts are compared using the Urbain method based on slag mineral composition and temperature.[4] Calculated slag viscosity is expressed in units of milli Pascals per second (mPas). A value of 5000 mPas or lower gives a free flowing slag.

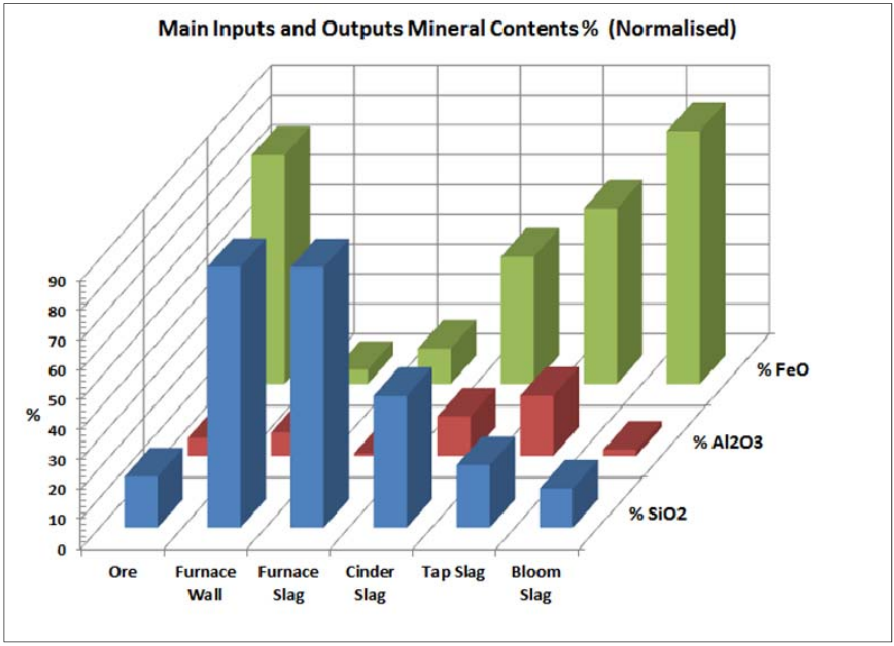

Figure 7 – Smelt 8 - Main Minerals re-distribution during Smelt

Higher lime and magnesia proportions in slag, giving higher basicity, reduce viscosity whereas increasing proportions of silica and alumina, giving lower slag basicity, increase slag viscosity. This ratio of proportions for these two mineral groups provides the (B_2) measure for slag basicity. Slag basicity and temperature influence viscosity.

Additionally the Urbain model shows slag becomes more fluid as wüstite proportion increases, as happens during Stage 2 reduction. However, during Stage 3 reduction slag viscosity increases from progressively reducing wüstite content and the presence of an increasing proportion of iron particles. These changing viscosities influence the rate of iron particles merging and growth, their drop rate in furnace and so bloom formation rate.

Viscosities and Influences on Bloom Formation

Low viscosity slags enable nucleated iron crystallites (specific gravity around 7.7 compared with fayalite slag at about 4.4) to gravitate and

aggregate more easily to form a bloom - usually below furnace tuyere level. Bloom growth now depends on a continuous supply of accreting iron particles and globules descending easily through a fluid slag. Table 1 includes smelt average iron drop rate.

At prevailing temperatures (850°C–1100°C+) created iron particles in liquid slag are solid and likely to absorb carbon by diffusion from the reaction of newly formed iron with carbon monoxide ($3Fe + 2CO \rightarrow Fe_3C + CO_2$). This is especially so when operating the furnace at high $CO:CO_2$ ratios (as for these smelts using high quality charcoal) and if furnace temperature is in the lower region. Iron, descending slowly in a viscous slag, has a longer 'residence time' during which to become carburised in this way and for small particles especially, to reach quickly a high carbon content. Small zones in a sample of smelt 10 bloom slag iron each had a different carbon content (range 0.06%C – 0.61%C and average 0.3%C) suggesting localised variable viscosities, variable carbon pick-up and so variable drop rates. A sample from smelt 9 forged billet showed 0.42% carbon content in iron (indicating medium carbon steel) and as to be shown shortly, a more viscous tap slag from some silica pick-up, slightly lower wüstite percentage and lower furnace temperature confirmed from smelt report.

Local slag viscosities are dynamic and a common controlling factor for these interdependent processes. Whilst Urbain equations provide a basic viscosity value for a slag composition and temperature, a value may need to be adjusted as now described.

Effect of Metallisation

Table 6 shows the metallisation effect by comparing sample smelt 8 and 10 cinder slags viscosities before and after metallisation. Metallised compositions are normalised and viscosities recalculated.

As an example Fig. 8 compares calculated temperature/viscosity profiles for smelt 10 cinder slag before and after metallisation.

Smelt 8 slag shows a similar profiles relationship although viscosity values are significantly higher from lower slag basicity. So lower viscosity smelt 10 cinder slag above 1100°C aided iron particle gravitation and bloom growth. Conversely for more viscous smelt 8 iron particle gravitation would take longer through cinder slag unless

Minerals \ Slag Type:	Smalt 8 Cinder Slag Sample %	Smelt 8 Metallised Cinder Slag %	Smelt 10 Cinder Slag Sample %	Smelt 10 Metallised Cinder Slag %
Metallised Iron Wt.%	0	20.00	0	30.00
Total Iron in Slag	30.41	10.41	38.13	8.13
FeO	39.11	18.69	49.04	17.34
Silica	40.57	56.57	28.1	46.59
Alumina	12.10	16.87	3.42	5.67
Lime	3.36	4.69	12.59	20.88
Magnesia	1.92	2.68	5.74	9.52
Manganese as MnO	0.38	0.53	0	0
Reduction % =	**0%**	**76%**	**0%**	**85%**
Slag Deg. C	**Viscosity mPas**	**Viscosity mPas**	**Viscosity mPas**	**Viscosity mPas**
1100°C	43377	1556000	3357	12108
1200°C	14832	352434	1539	4721
1300°C	5838	96812	782	2084
1400°C	2579	31154	433	1018
1500°C	1253	11431	257	541
1600°C	660	4683	162	309
Basicity		0.10		0.58

Table 6 – Effect on smelt 8 and smelt 10 Cinder Slag Viscosities from formation of Metallised Iron

temperature was increased significantly. Smelt 8 gross bloom yield was about 32% compared with about 71% yield for smelt 10.

Hindered Settling

Hindered settling occurs when dispersed iron particles create a more viscous slag. Unlike compositional change from metallisation, hindered settling is a physical result of particulate concentration.[5] Fig. 9 shows a basic Einstein-Roscoe factor effect of iron particles volume fraction on slag viscosity following nucleation and aggregation.

Around 18% particulate volume fraction is sufficient to double slag viscosity. To offset just this effect alone to regain original viscosity for smelt 10 slag would require a furnace temperature increase from around 1100°C to 1200°C (see previous Table 6).

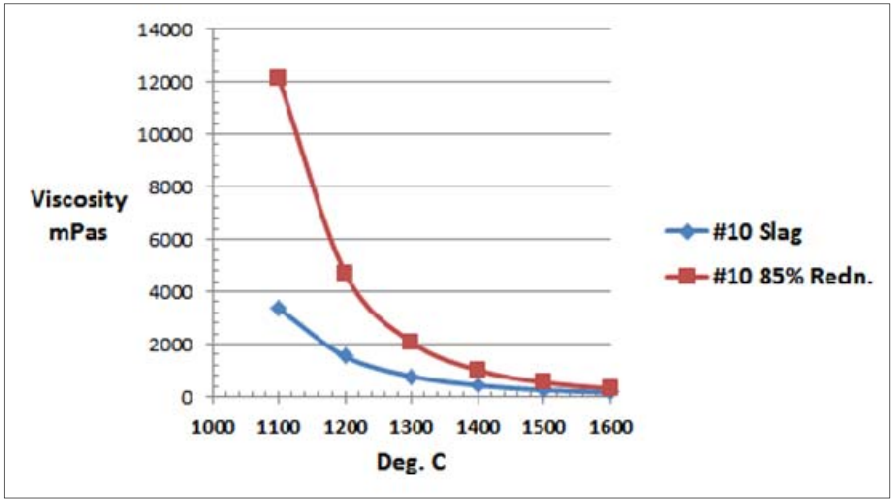

Figure 8 – Viscosities for smelt 10 Cinder Slag before and after 85% Reduction

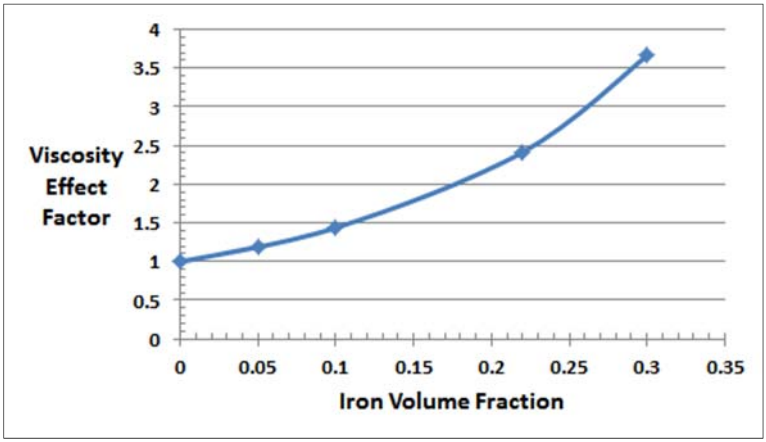

Figure 9 – Effect of Iron Particles Volume Fraction on Slag Viscosity

Particle Settlement

Bloom growth from iron settlement rate can be compared broadly using *basic principles* of Stokes Law. Fig. 10 illustrates the type of situation by comparing velocity profiles of regular iron particles of different sizes falling under gravity through slag of different viscosities. Like hindered settlement this is a physical effect and might be affected by upward flow force of gases on small particles.

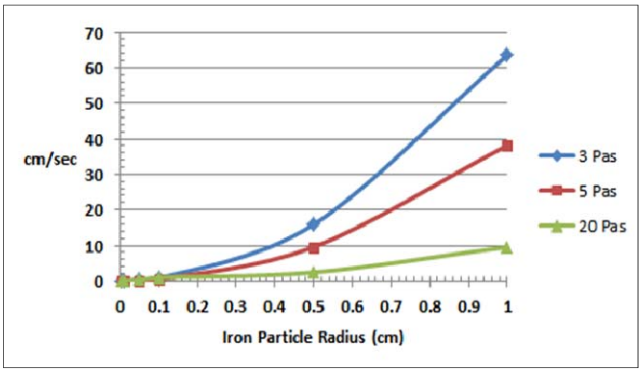

Figure 10 – Comparing Drop Rates for Iron Particles in different viscosity Slags

(Note: 1 Pas = 1000 mPas)

As particles grow this shows how drop rate for a size declines as viscosity increases giving longer residence time for particles. However slag viscosity is variable locally and evolving from changing slag compositions and furnace zone temperatures. Even with charcoal present, likely causing some flow resistance, Fig. 10 shows that small iron particles could fall easily several centimetres in a few seconds through low viscosity slag.

Bloom Growth

On reaching the hearth zone globules and slag are likely eddied by sloping tuyere air stream forces into a liquid slag pool where heavier iron settles in a less active zone below the tuyere. Here iron globules fuse building steadily a bloom mesh in a protective liquid slag bath (+charcoal). Furnace tapping releases built up bloom slag as tap slag.

Tap Slag Characteristics

In the hearth zone a slag viscosity of 5000mPas or lower enables good slag separation from bloom iron formation. Table 7 compares smelt tap slag wüstite proportions (by metallography). A lower wüstite percentage indicates higher smelting efficiencies but a higher viscosity. A compromise is likely to exist between having good furnace reduction efficiency and getting good tap slag separation from the bloom. An increase in tapping temperature would help reduce viscosity.

Smelt	Wüstite %	Observed Flow
8	15	Good flow
9	14	Initial small sample flow
10	18	Copious flow of fluid slag

Table 7 – Percentage Wüstite in Smelt Tap Slag and Flow Type

Mineral Contents

Mineral contents for tap slags, Fig. 11, show a fairly consistent value for total FeO. However comparative effects of mineral differences on a tap slag viscosity profiles are shown in Figure 12. Especially notable is the effect of temperature on viscosity.

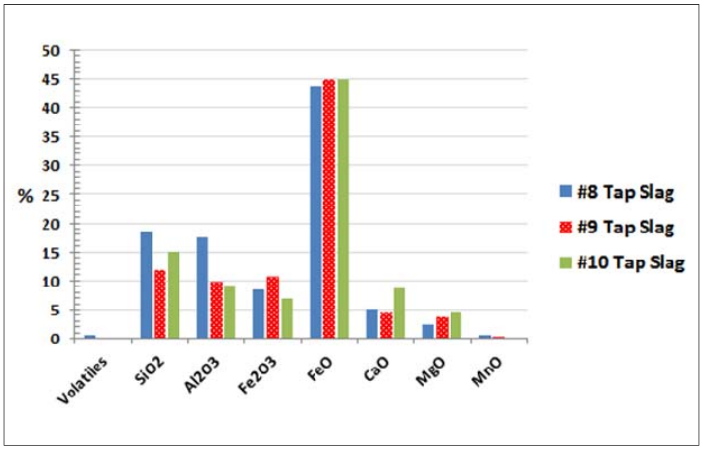

Figure 11 – Comparison of Tap Slags Mineral Contents

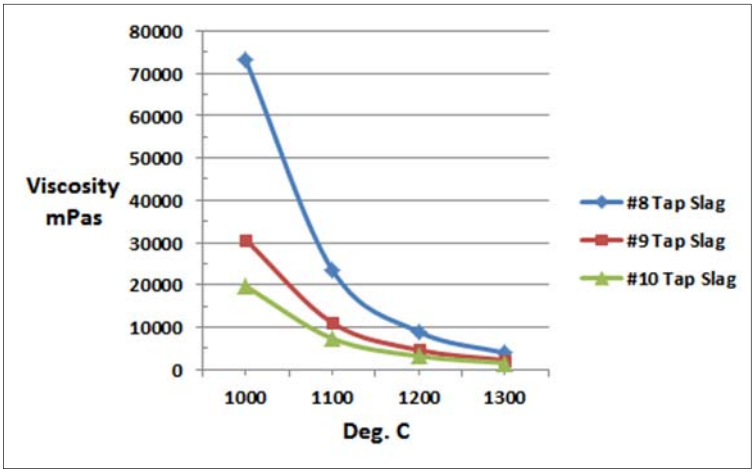

Figure 12 – Viscosity Profiles for Smelt Tap Slags against Temperature

Fig. 13 shows relative temperatures and critical viscosity of 5000mPas for a good tap slag flow.

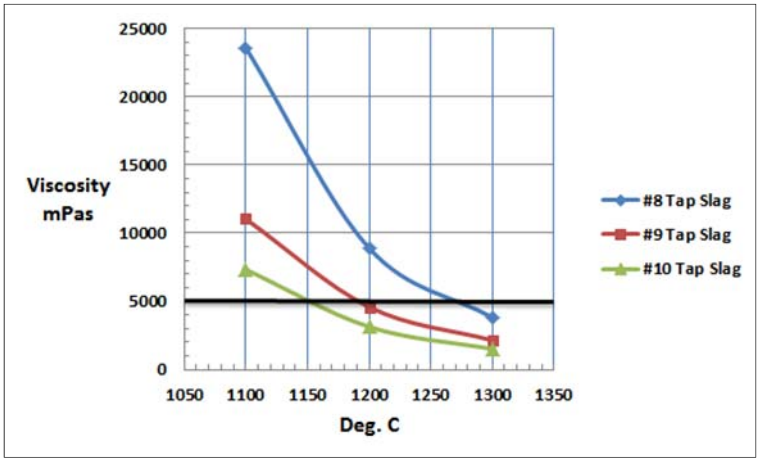

Figure 13 – Viscosities and Critical Flow Temperatures for Tap Slags

At 1280°C all tap slags should have been fluid for tapping. However:

- smelt 8 tap slag was especially sensitive to temperature whereby a slightly lower temperature of just 1250°C would render this slag more difficult to tap easily. The smelt gave a good tap slag flow indicating hearth temperature achieved critical viscosity value

- smelt 9 tap slag did not flow after a small initial quantity. Probing gave a sticky slag on the probe tip even though a useful bloom yield was achieved. Whilst 1200°C should have been adequate for tapping flow, either a) the tapping outlet was misaligned, or more likely b) hearth temperature was marginally low

- smelt 10 produced the lowest viscosity tap slag and good flow. This is attributed to a quantity of retained ash in the hearth increasing slag basicity and so fluidity.

Smelt 10 Anomaly

Earlier in this article three key 'unplanned' events were described which in some way helped achieve an impressive bloom yield of 71%. How each could have influenced this outcome is explored:

Effect of Lime in Wood Ash on Ore Reduction Rate

Various ore reducibility trials, such as described by Bollina *et al* and by Khedr and Abdel-Khalik,[6,7] show how haematite (Fe_2O_3) ore reduction rate depends on temperature and especially burden mix basicity. Based on published data lime addition, giving a basicity of 0.7 (similar to that for smelt 10), lowers reduction activation energy for a temperature compared with unlimed ore. Fig. 14 shows how reaction rate constant values vary with temperature for limed and unlimed ores. A higher rate constant value for a limed ore enables a higher bloom iron formation rate (gms/min) and so final bloom yield within smelt time.

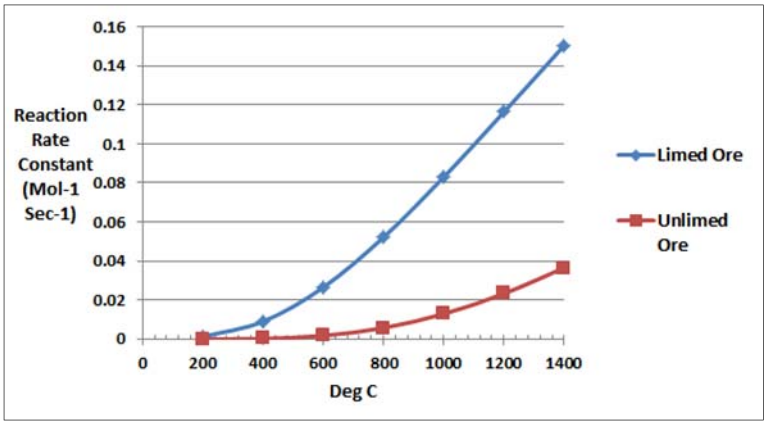

Figure 14 – Comparison of Effects of Liming and Temperature on Iron Ore Reduction

Effects of Lime Releasing Iron from Fayalite

Lime as CaO can combine with silica, in preference to FeO in fayalite, to form calcium silicate and less fayalite in slag. This gives extra FeO for Stage 3 reduction to bloom iron. Moreover an 80% fayalite + 20%

calcium silicate mix slag has a lower viscosity and melting point of around 1117°C, compared with that for fayalite slag which is closer to 1200°C. Estimated tap slag flow temperature for smelt 10 was around 1150°C (Fig. 13).

Repositioned Tuyere & Air Flow Disruption

As well as these effects it seems that repositioning the tuyere could have contributed to a better formed hot furnace zone enabling more iron production. Finally additional effects of short term tuyere air flow disruption, thereby removing any counter flow effects followed by lower flow rate hand bellowing, gave additional time for iron to drop and consolidate for a higher yield.

These effects in combination allowed more iron to form a bloom more effectively within the low viscosity, higher basicity smelt 10. Figure 15 shows the overall empirical relationship for these smelts for an average iron drop rate over smelt duration and slag basicity.

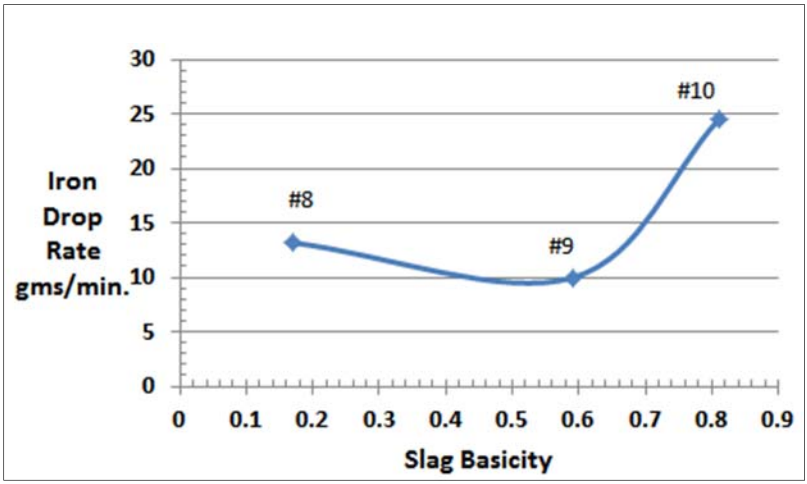

Figure 15 – Smelt Slag Basicity and Iron Drop Rate

Influence Map

Findings from these three smelts show the effects of many interacting factors affecting final bloom yield when starting from a notionally

common burden specification and mix. From these interactions an *Influence Map,* Fig. 16, has been created. This shows these dependency links and how changes between levels for inputs, smelting processes and intermediate outputs affect final bloom yield especially for Stage 3 reduction to iron.

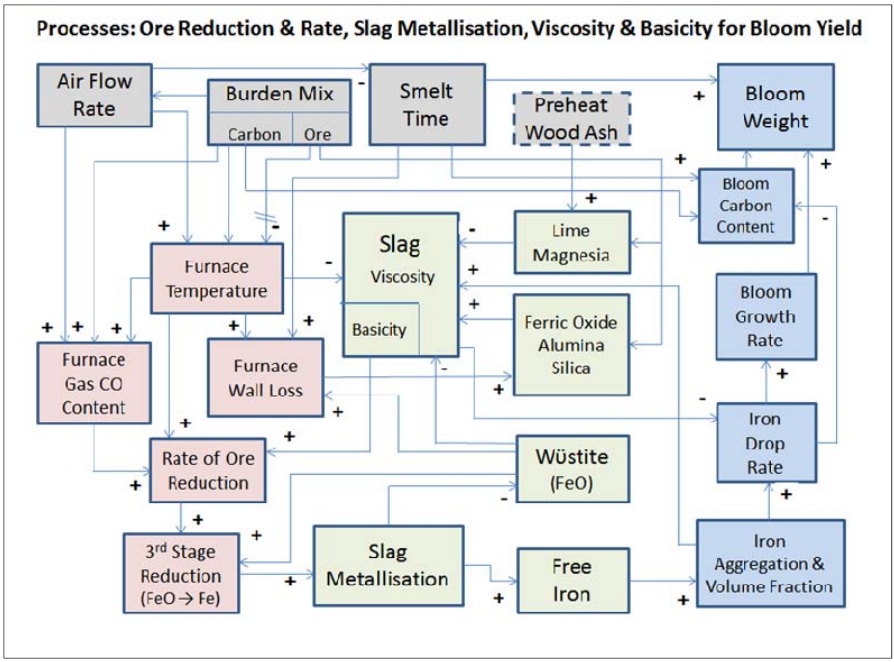

Figure 16 – Process Factors Influencing Slag Properties and Bloom Formation

(NOTE: '+' Supportive effect on; '-' Inverse effect on, '//' Delay effect on)

Sequential links demonstrate how changes in furnace inputs (top left section) ripple through the system and interact along 'pathways' via furnace operations (left hand side), slag viscosity and basicity (centre section), metallisation and bloom formation (lower section) to influence final bloom yield and carbon content (right hand side). Variations in final bloom yields can be aligned to relative differences or changes from

starting conditions, pathways followed and feedback effects for each smelt.

Conclusions

Even starting with notionally the same burden mix and similar smelting plan each smelt still produced a markedly different bloom yield and carbon content. Analyses show the influential importance for yield of temperature on slag viscosities during metallisation and bloom forming. This was seen especially when comparing smelts 8 and 9, both of which avoided events affecting smelt 10. Unplanned as events were for smelt 10 its outcomes gave the opportunity to explore and show how the effects of lime additions, lower slag viscosities and changed air flow rates can be associated with increased bloom yield. Also how a range of 'normal' smelting outcomes can mask effects of other operational changes.

Temperature management of furnace zones, aligned to burden mineral contents and stage of reduction, is crucial for achieving slag viscosities for good bloom building and tap slag separation. The *Influence Map* offers a tool that can help identify key pathways and factors for achieving these and importantly, be validated or modified against further smelting trials and findings.

References

1. Gupta, R. C, 2010, *Theory and Laboratory Experiments in Ferrous Metallurgy* (New Delhi, Prentice Hall of India), Chapter 9.5.

2. Davies, A. F., 2015, 'Genesis of Bloomery Iron – A Note', *Wealden Iron*, Bulletin of the Wealden Iron Research Group, 2nd ser., **35**, 31-32.

3. Wagner, D., Devisme, O., Patisson, F. and Ablitzer, D., 2008, 'A laboratory study of the reduction of iron oxides by hydrogen', in F. Kongoli and R.G. Reddy (eds.), *Proceedings of the Sohn International Symposium, 27-31 August 2006, San Diego*, TMS, **2**, 111-120.

4. www.algoness.co.za, 'tool-calculate-slag-liquid-viscosity-silverlight 8 Nov 2010' - A general model based on the Urbain formalism providing

viscosity calculations in Microsoft Excel

5. Migas, P., Korolczuk-Hejnak, M., Karbowniczek, M., 2012, 'Rheological Analysis of Blast Furnace Synthetic Slag Admixtures of Al2O3', Department of Ferrous Metallurgy, Faculty of Metal Engineering and Industrial Computer Science, AGH-University of Science and Technology, 30-059 Krakow, Poland. Extracted from: www.pyrometallurgy.co.za, Molten Slags 2012, W173.pdf

6. Bollina, R., Sharma, S. K., Mishra, V. K., Shubhakar, N. E. P., Roshan, V., Deogade, B. K., Vijayalakshmi, K. and Narayana, P. V. S. L., 2013, 'Effect of Lime Coating of Iron Ore Pellets on Iron Production', Department of Metallurgical and Materials Engineering, Mahatma Gandhi Institute of Technology, Gandipet Hyderabad-500075, AP, India. Technical Paper for Conference MPT 2013, Bhubhaneshwar, 10-12 December 2013.

7. Khedr, M.H., Abdel-Khalik, M H., 1996, 'Study on Using Dolomite instead of Limestone as Fluxing Material During Sintering Process and its Effect on the Reduction and Mechanisms', *Fizykochemiczne Problemy Mineralurgii*, **30**, 135-144.

INDEX

Ashdown Beds, 3

Battle (East Sussex)
  Beauport Park, 12
bloomeries, 3, 12
  blowing, 22
  charging, 22
  furnace lining, 7, 9, 10, 20-8
  tapping, 22
  yields, 20-8, 29-49

charcoal, 23

Davies, A. F., 20, 29

English, J., 3

hammerscale, 15-17

Iron Age, 7, 11
iron bloom, 43
  carbon content, 31
  formation, 48
iron ore, 9, 20
  reduction, 31-2, 46
  roasted, 15, 17, 20, 23
iron slag, 7, 13, 14-17, 20, 23
  calcium in, 15
  fayalite, 46-7
  manganese in, 15
  metallisation, 33-4, 39
  morphology, 16
  silicon in, 15
  types, 32-7, 43
  viscosity, 37-9, 42, 44-5
  wüstite, 20-1, 34

Lea, D., 3

Manaton (Devon)
  Kestor Iron Age site, 11, 12

paludina limestone, 9
pottery, 7
  Iron Age, 7
  medieval, 7
  Romano-British, 12
Prus, J. L., 3

Roman, 12
Rotherfield (East Sussex)
  Minepit Wood bloomery, 12

Salehurst (East Sussex)
  Lordship Wood, 3
  Robertsbridge Abbey, 13
  Scott's Hollow bloomery, 3-18
  Wellhead Wood, 3
Sedlescombe (East Sussex)
  Footland Farm, 14
  'cinder beds', 13
  Oaklands Park, 12
smithing, 27

Tunbridge Wells Sand, 3
tuyere, 29, 31, 47

Wadhurst Clay, 3